Electronic Supplementary Material (ESI) for ChemComm.

Regioisomeric cryptands stabilized gold suprasphere and elongated dodecahedron supraparticle for reversible host-guest chemistry

Meenaxi Saini,[a] Ashish Verma,[b] Kapil Tomar,[b] Parimal K. Bharadwaj,*[b] and Kalyan K. Sadhu*[a]

[a] Department of Chemistry, Indian Institute of Technology Roorkee, Roorkee – 247667, Uttarakhand, India

[b] Department of Chemistry, Indian Institute of Technology Kanpur, Kanpur - 208 016, Uttar Pradesh, India

Supporting Information

Experimental detail

Materials

For the gold nanoparticles, the chemicals gold (ш) chloride trihydrate was purchased from Sigma-Aldrich, trisodium citrate dihydrate was purchased from Merck Chemicals, 4-(diethylamino)salicylaldehyde and ethylcyanoacetate were purchased from TCI India, piperidine was purchased from Alfa Aesar, ethanol was purchased from Finar Limited and diethyl ether was purchased from Himedia. All glassware were cleaned with aqua regia (mixture of 1:3 volume ratios of HNO_3 and HCl) and rinsed with Millipore water prior to use.

Synthesis of cryptands1-2

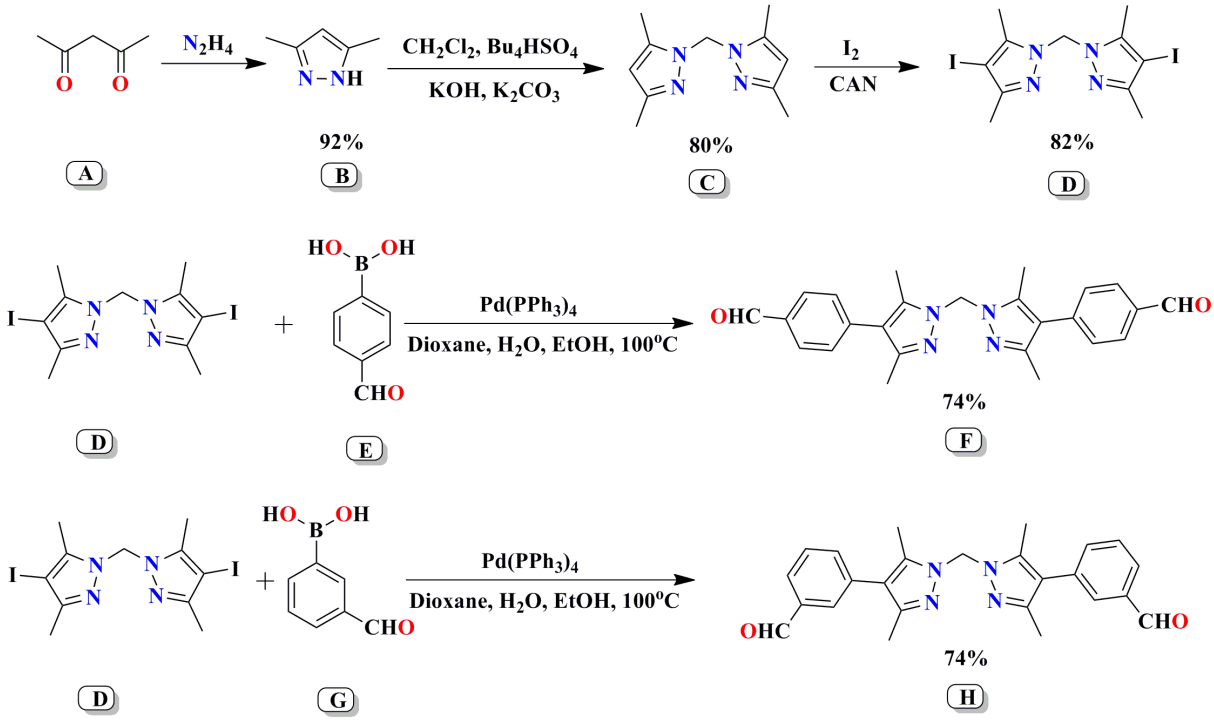

Synthetic scheme for preparation of dialdehyde **F** and **H**

Synthesis of dialdehyde F and H

Synthesis of dialdehyde F

Mixture of 4-formylphenylboronic acid (1.45 g, 9.64 mmol, 2.2 equiv), compound **D**[S1] (2 g, 4.38 mmol, 1.0 equiv), $Pd(PPh_3)_4$ (254 mg, 0.219 mmol, 0.05 equiv) and K_3PO_4 (3.72 g, 17.54 mmol, 4 equiv) in 90 mL of dioxane/distilled H_2O/EtOH (6/2/1, v/v/v) was stirred under nitrogen atmosphere for 72 h at 100 °C. After the mixture was cooled to room temperature, the reaction mixture was poured into distilled water and aqueous phase was extracted with CH_2Cl_2. Evaporation of the solvent followed by purification using column chromatography (silica gel; ethylacetate/hexane = 40:60) afforded 0.85g of **F** as yellowish solid. Yield: 74%. ^1H NMR (400 MHz, $CDCl_3$, 25 °C, $Si(CH_3)_4$): δ= 10.00 (s, 2H), 7.92 (d, 4H), 7.41 (d, 4H), 6.22(s, 2H), 2.57 (s, 6H), 2.26 (s, 6H).

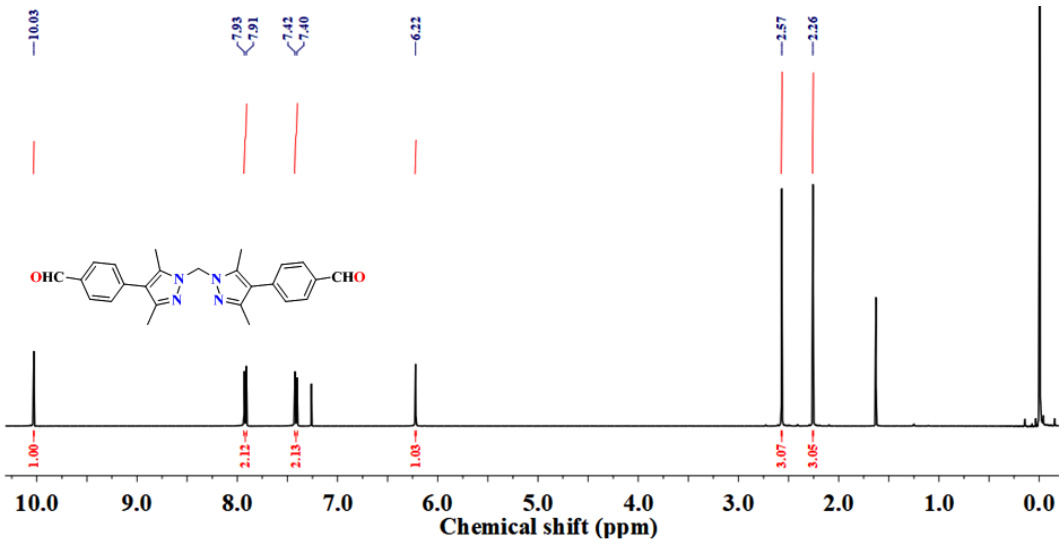

^{1}H NMR spectrum of dialdehyde **F**

Synthesis of dialdehyde H

Synthesis of dialdehyde is same as **F** except 3-formylphenylboronic acid is used in place of 4-formylphenylboronic acid. Yield: 68%. ^{1}H NMR (400 MHz, $CDCl_3$, 25 °C, $Si(CH_3)_4$): δ= 10.05 (s, 2H), 7.81 (d, 2H), 7.76 (s, 2H), 7.58 (t, 2H), 7.52 (d, 2H), 6.25 (s, 2H), 2.53 (s, 6H), 2.24 (s, 6H).

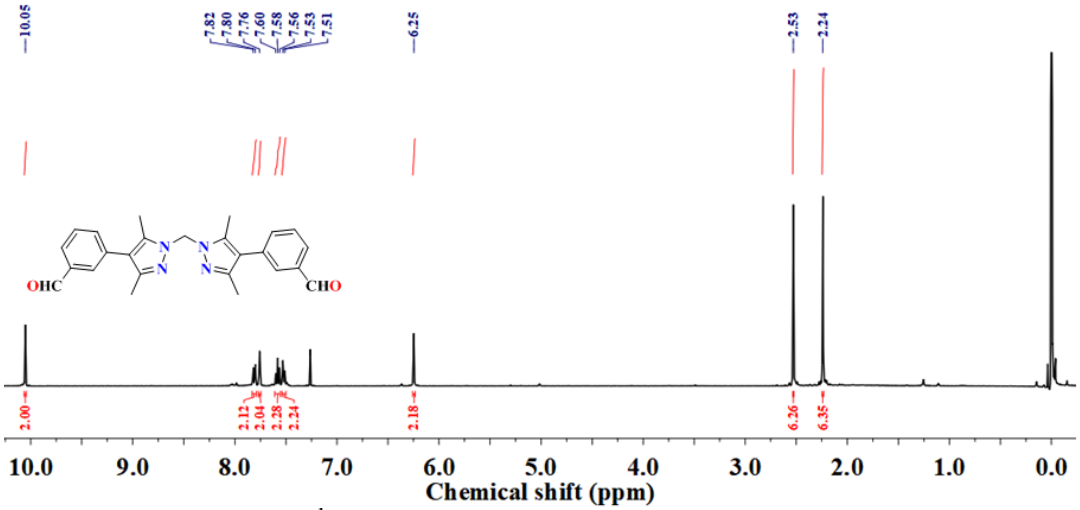

^{1}H NMR spectrum of dialdehyde **H**

Synthesis of 1,2,3-Tris(aminomethyl)-2,4,6-trimethylbenzene

The aromatic triamine was synthesized by following the reported procedures.[S2, S3]

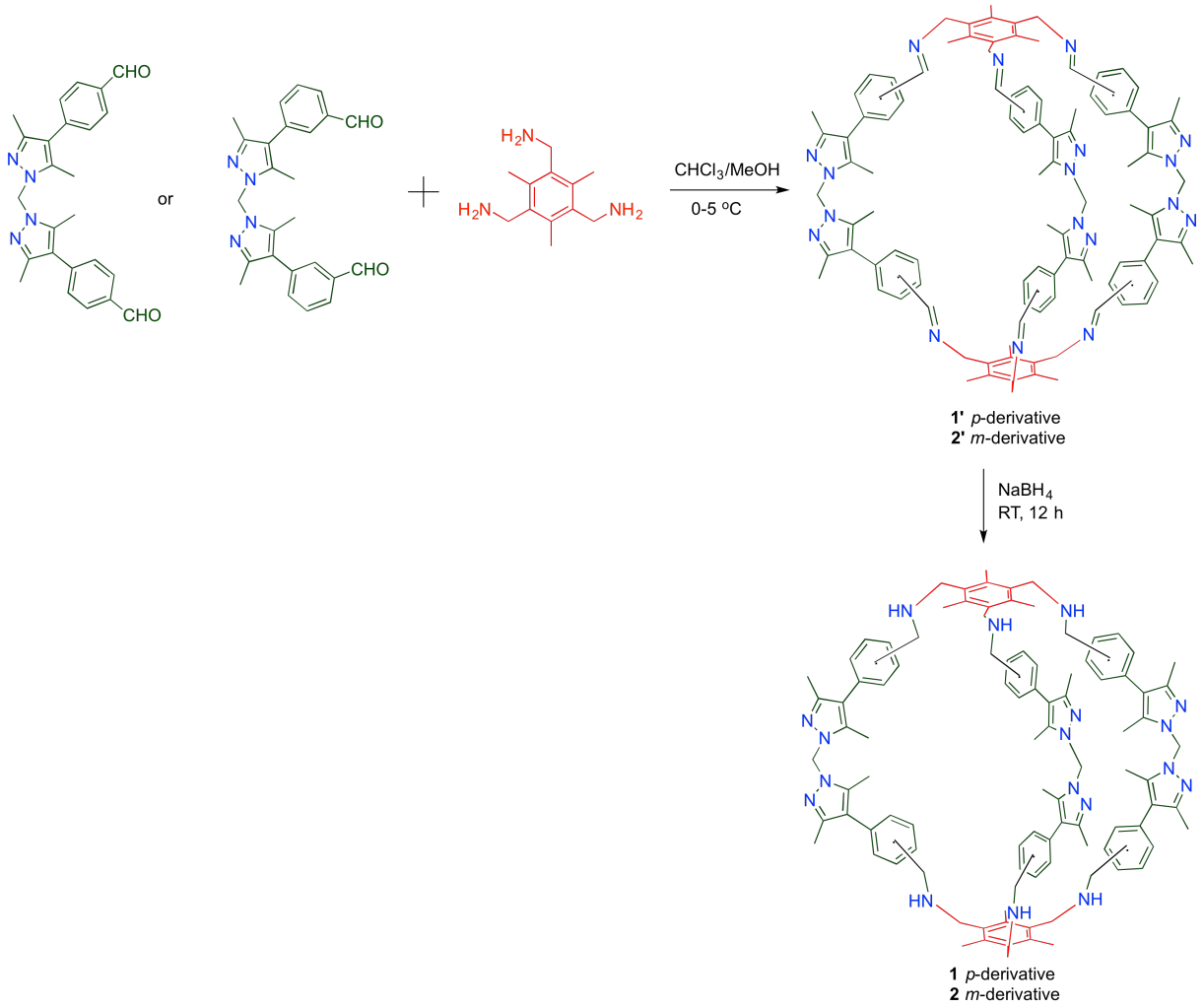

Syntheses of imine cryptands (**1'** and **2'**) and imine cryptands (**1** and **2**).

Synthesis of Cryptand 1

A solution of dialdehyde **F** (700 mg, 1.7 mmol) is taken in $CHCl_3$-MeOH (1:1 v/v, 400mL) in a 1 L round bottom flask at 5ºC. To this solution is added, with continuous stirring a solution of 1,2,3-tris(aminomethyl)-2,4,6-trimethylbenzene (233 mg, 1.12 mmol) in MeOH (150 mL) over a period of 12 h and stirred for further 12 h. The temperature is maintained at 5±1 ºC and the addition is so adjusted that a drop disperses completely before another drop can fall into the reaction mixture. After the addition is complete a clear solution is formed. Then excess of solid $NaBH_4$ (≈ 200 mg) is added in portion and stirred 12 h. After complete removal of the solvent, the white solid left is extracted with $CHCl_3$ and washed with water (2 × 200mL). The organic layer is dried over Na_2SO_4 and solvent is completely removed to obtain **1** as a white solid. Yield: 68%. ^{1}H NMR (400 MHz, $CDCl_3$, 25 °C, $Si(CH_3)_4$): δ= 7.41 (s, 2H), 7.39 (s, 3H), 7.35 (s, 4H), 7.33 (s, 4H), 7.24 (s, 2H), 7.23 (s, 2H), 7.14 (s, 4H), 7.12 (s, 3H), 6.15 (s, 6H), 3.89 (d, 24H), 2.50 (s, 9H), 2.47 (d, 27H), 2.15 (s, 18H).^{13}C NMR (400 MHz, $CDCl_3$, 25°C, $Si(CH_3)_4$): δ (ppm) = 153.40, 146.64, 138.99, 137.62, 136.77, 133.17, 129.77, 127.27, 120.12, 65.30, 61.09, 12.70, 10.56. ESI-MS: m/z 1556.9586 $[M+H]^+$; calculated: m/z 1556.9600 $[M+H]^+$. CCDC No. 1836525; FTIR (KBr) υ/cm^{-1}: 3389, 2920, 2859, 2216, 1667, 1615, 1575, 1512, 1434, 1375, 1331, 1303, 1240, 1101, 1031, 1011, 858, 819, 724, 691, 626, 589, 563, 505.

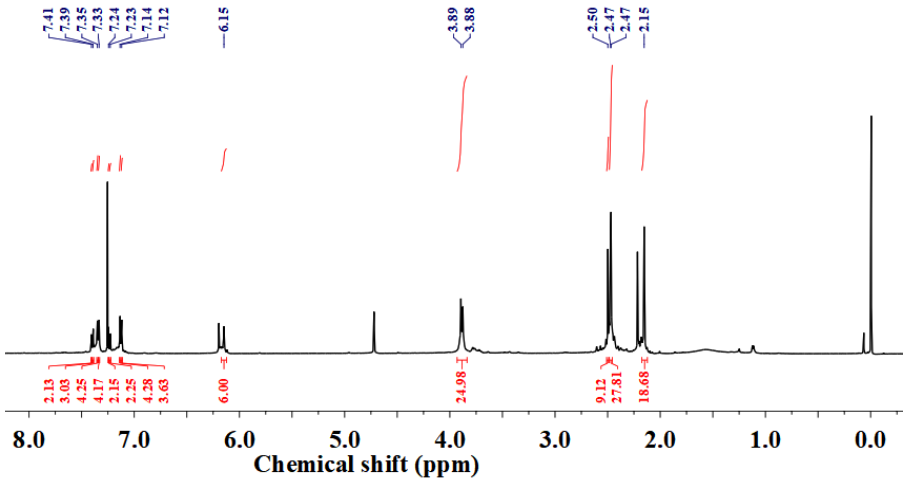

^{1}H NMR spectrum of Cryptand **1**

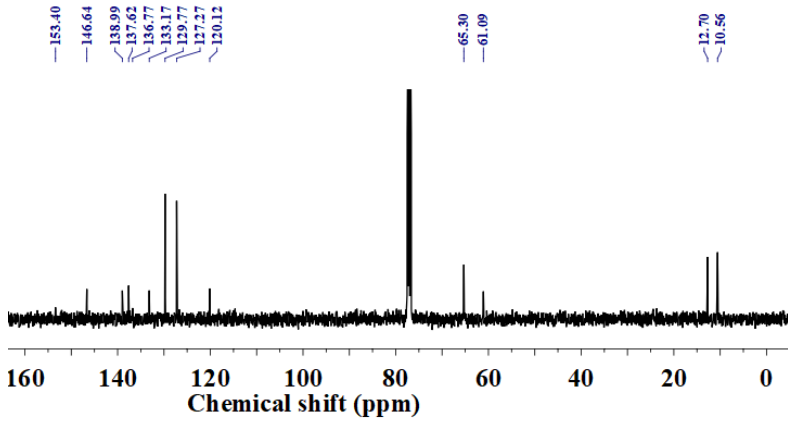

^{13}C NMR spectrum of Cryptand **1**

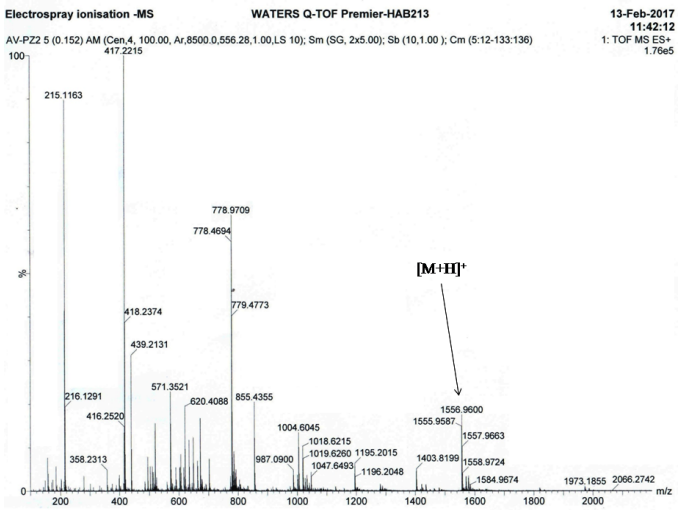

ESI-MS spectrum of cryptand **1**

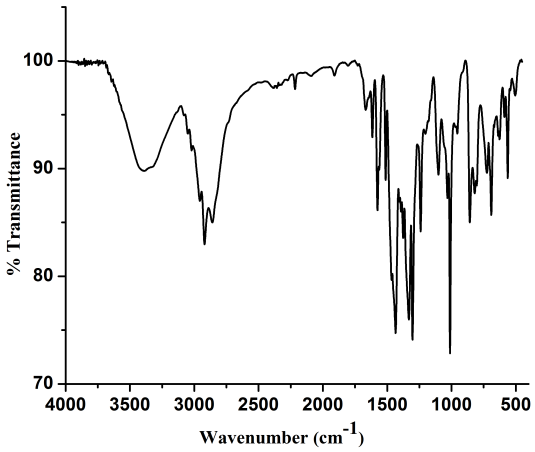

IR spectrum of Cryptand **1**

Crystallographic data

Cryptand 1	
Formula	$C_{99}H_{114}N_{18}$
M_w (g mol^{-1})	1556.09
Crystal system	Triclinic
Space group	*P*-1
a (Å)	16.1763(9)
b (Å)	20.0396(11)
c (Å)	21.3747(12)
α (°)	66.358(10)
β(°)	76.628(2)
γ(°)	78.423(2)
V (Å^3)	6129.9(6)
Z	2
ρ_{calcd} (g cm^{-3})	0.843
μ(MoKα) (mm^{-1})	0.051
F(000)	1668
Collected reflections	22766
Independent reflections	10291
Goodness-of-fit (GOF) on F^2	1.065
R1, wR2 ($I > 2\sigma I$)	0.0809, 0.2221
R1, wR2 (all data)	0.1672, 0.2624
CCDC Number	1836525

Synthesis of Cryptand 2

Synthesis of cryptand **2** is same as cryptand **1** except dialdehyde**H** is taken in place of **F**. Yield: 62%. ^{1}H NMR (400 MHz, $CDCl_3$, 25 °C, $Si(CH_3)_4$): δ= 7.35 (d, 7H), 7.32 (s, 2H), 7.30 (s, 2H), 7.29 (s, 1H), 7.21 (d, 3H), 7.16 (s, 3H), 7.13 (s, 4H), 7.11 (s, 2H), 6.35 (s, 6H), 3.97 (d, 12H), 3.67 (d, 12H), 2.41 (s, 18H), 2.20 (s, 18H), 2.12 (s, 18H). ^{13}C NMR (400 MHz, $CDCl_3$, 25°C, $Si(CH_3)_4$): δ (ppm) = 146.61, 145.91, 141.20, 137.62, 136.26, 134.02, 133.84, 128.88, 128.70, 128.13, 128.02, 126.46, 125.14, 121.74, 120.32, 65.31, 61.11, 54.26, 48.49, 29.78, 15.61, 12.69, 12.50, 10.56, 10.13. ESI-MS: observed: m/z 1556.9586 $[M+H]^+$; calculated: m/z 1556.9615 $[M+H]^+$. FTIR (KBr) υ/cm^{-1}: 3312, 2921, 2854, 1666, 1608, 1587, 1565, 1491, 1436, 1377, 1333, 1305, 1247, 1205, 1089, 1050, 907, 874, 790, 711, 662, 630.

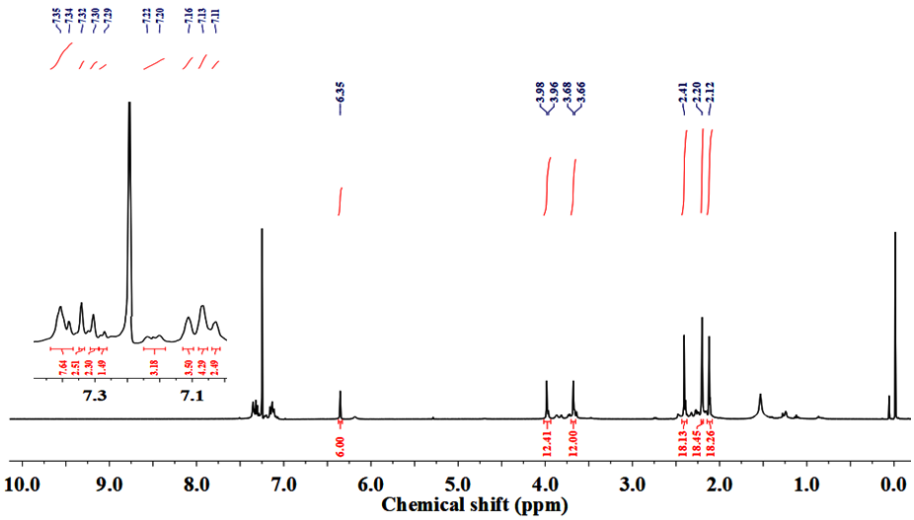

^{1}H NMR spectrum of Cryptand **2**

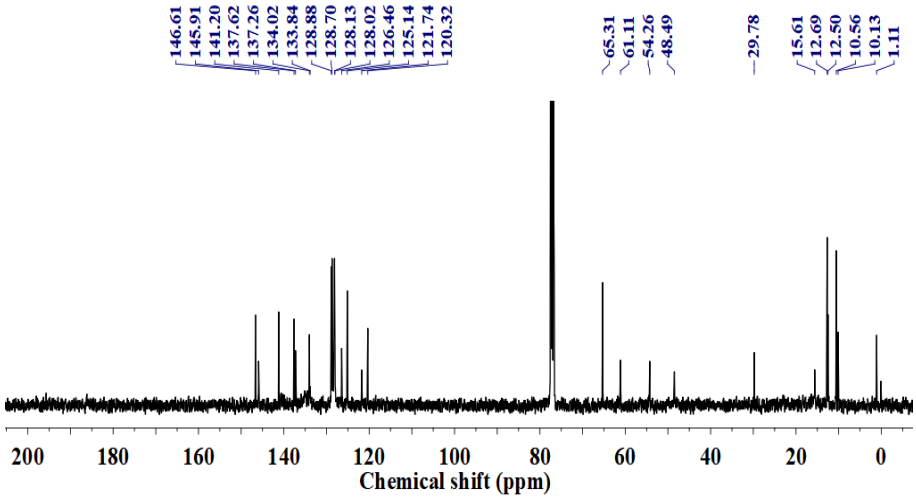

^{13}C NMR spectrum of Cryptand **2**

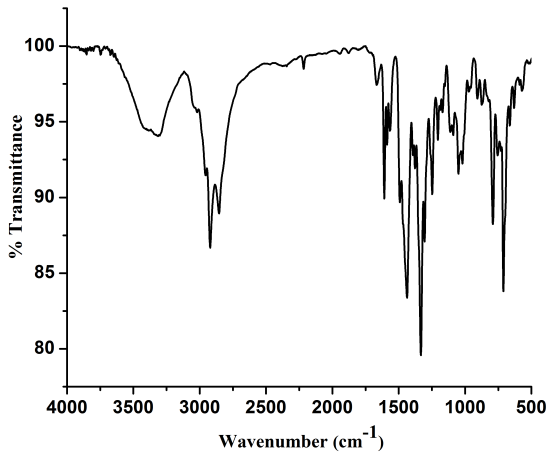

IR spectrum of Cryptand **2**

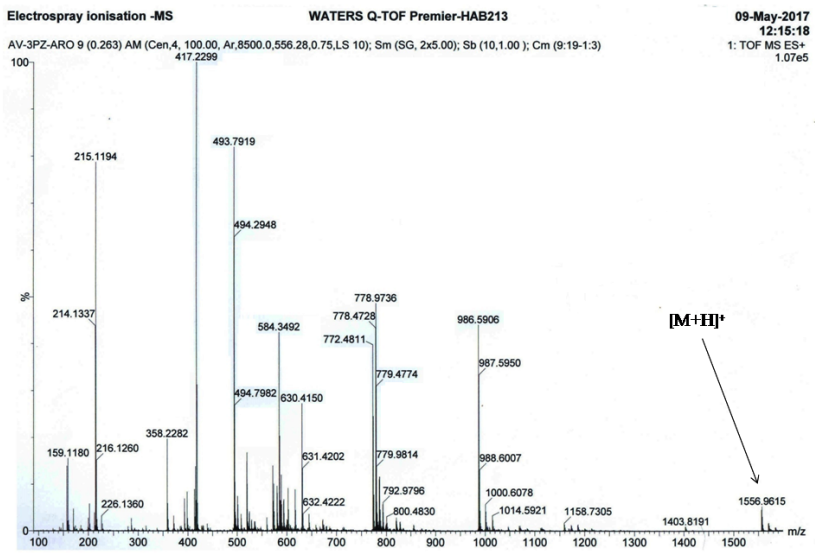

ESI-MS spectrum of cryptand **2**

Synthesis of AuNP

23.6 mg (0.05 mmol) of gold (III) chloride trihydrate was dissolved in 200 mL of Millipore water and boiled under reflux condenser with constant stirring. Then 57 mg (0.19 mmol) of trisodium citrate dihydrate was dissolved in 1.8 mL of millipore water and added to refluxing solution. After the addition, initially the solution was dark violet, which quickly changed to red. The reaction was allowed to continue for 30 min. The final gold nanoparticles were cooled to room temperature.

Synthesis of $AuSS_L$

39.6 mg (0.025 mmol) of **1** was dissolved in 2.5 mL DMSO and added to 50 mL **AuNP** solution. After 2 minutes shaking, the solid **$AuSS_L$** was isolated by centrifugation and the sample dried under vacuum.

Synthesis of $AuED_L$

38.9 mg (0.025 mmol) of **2** was dissolved in 2.5 mL DMSO and added to 50 mL **AuNP** solution. After 2 minutes shaking, the solid **$AuED_L$** was isolated by centrifugation and the sample dried under vacuum.

Synthesis of Au_1 (Au^{3+}:cryptand1 in 1:1 ratio)

4.7 mg (0.012 mmol) of gold (III) chloride trihydrate was dissolved in 40 mL of millipore water and 19.03 mg (0.012 mmol) of **1** was dissolved in 0.8 mL DMSO and added to gold (III) chloride trihydrate solution and boiled under reflux condenser with constant stirring. Then 11.4 mg (0.038 mmol) of trisodium citrate dihydrate was dissolved in 0.36 mL of millipore water and added to refluxing solution. After the addition, initially the solution was dark violet, which quickly changed to red. The reaction was allowed to continue for 30 min. The final gold nanoparticles were cooled to room temperature. The solid was finally isolated by centrifugation and the sample dried under vacuum.

Synthesis of $AuSS_{NL}$ (Au^{3+}:cryptand1 in 1:1.6 ratio)

4.7 mg (0.012 mmol) of gold (III) chloride trihydrate was dissolved in 40 mL of millipore water and 30.4 mg (0.019 mmol) of **1** was dissolved in 1.86 mL DMSO and added to gold (III) chloride trihydrate solution and boiled under reflux condenser with constant stirring. Then 11.4 mg (0.038 mmol) of trisodium citrate dihydrate was dissolved in 0.38 mL of millipore water and added to refluxing solution. After the addition, initially the solution was dark violet, which quickly changed to red. The reaction was allowed to continue for 30 min. The final gold nanoparticles were cooled to room temperature. The solid was finally isolated by centrifugation and the sample dried under vacuum.

Synthesis of $AuLS_{NL}$ (Au^{3+}:cryptand2 in 1:1.6 ratio)

4.72 mg (0.012 mmol) of gold (III) chloride trihydrate was dissolved in 40 mL of millipore water and 29.62 mg (0.019 mmol) of **2** was dissolved in 1.86 mL DMSO and added to Gold (III) chloride trihydrate solution and boiled under reflux condenser with constant stirring. Then 11.4 mg (0.038 mmol) of trisodium citrate dihydrate was dissolved in 0.36 mL of millipore water and added to refluxing solution. After the addition, initially the solution was dark violet, which quickly changed to red. The reaction was allowed to continue for 30 min. The final gold nanoparticles were cooled to room temperature. The solid was finally isolated by centrifugation and the sample dried under vacuum.

Synthesis of SEA-SC1

4-(diethylamino)salicylaldehyde (60 mg, 0.3mmol) and ethylcyano acetate (0.638 mL, 6 mmol) were dissolved in ethanol solution (3.5 mL). Piperidine (0.4 mL) was added and the solution was stirred at room temperature for 5 h. The solution was kept in fridge for 12 h. A yellow precipitate of **SEA-SC1** was observed. The precipitate was filtered, washed with diethyl ether and dried under vacuum (75 mg, y. 68 %). ^{1}H NMR ($CDCl_3$, 400 MHz) δ 1.24 (t, 6H), 1.35 (t, 3H), 3.46 (q, 4H), 4.27 (q, 2H), 6.47 (s, 1H), 6.64 (d, 1H), 7.40 (d, 1H), 8.46 (s, 1H); ^{13}C NMR (DMSO-d_6, 100 MHz) δ 12.5, 14.0, 14.6, 44.4, 59.9, 62.2, 71.3, 96.4, 106.7, 109.8, 113.8, 118.8, 130.7, 145.1, 152.0, 157.0, 158.2, 165.8, 167.2; LC-MS (ESI): RT = 3.52 min, m/z found: 356.4015; M.W. $[C_{19}H_{22}N_3O_4]^+$: 356.4000 $[M+H]^+$; FTIR (KBr) ν/cm^{-1}: 3410, 3160, 2210, 1693, 1629, 1526, 1405, 1277, 1199, 1140, 1096, 783, 611.

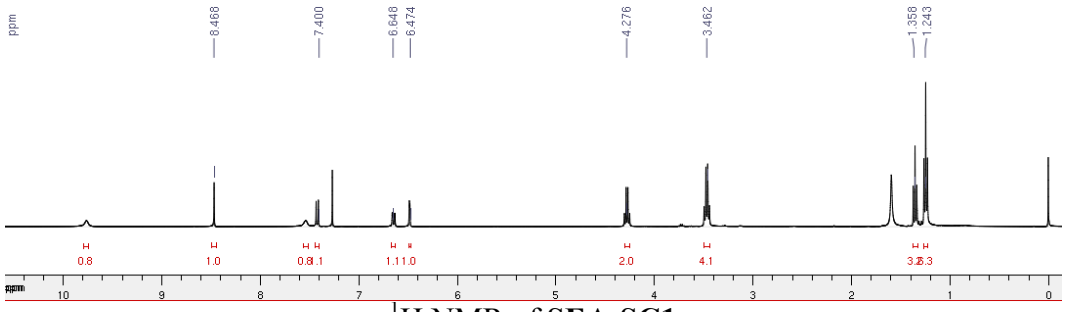

^{1}H NMR of **SEA-SC1**

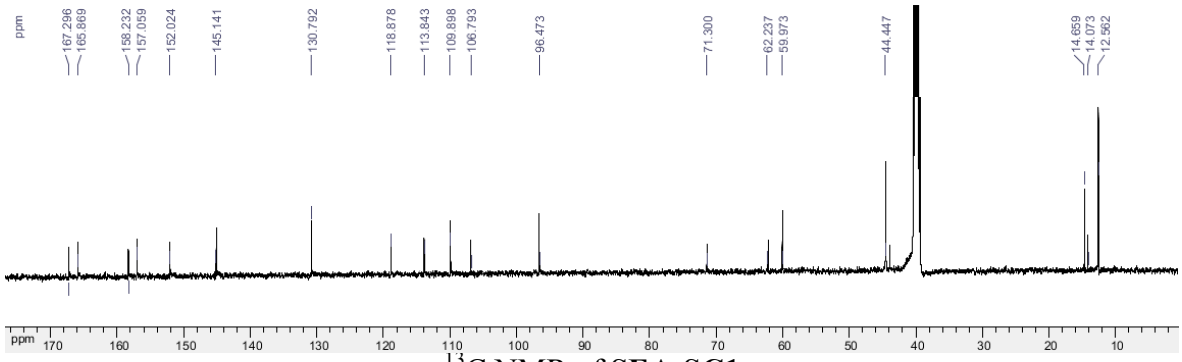

^{13}C NMR of **SEA-SC1**

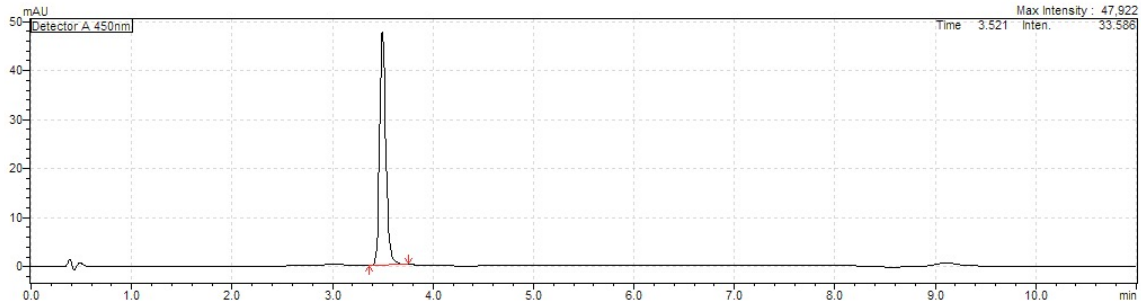

LC peak of **SEA-SC1**

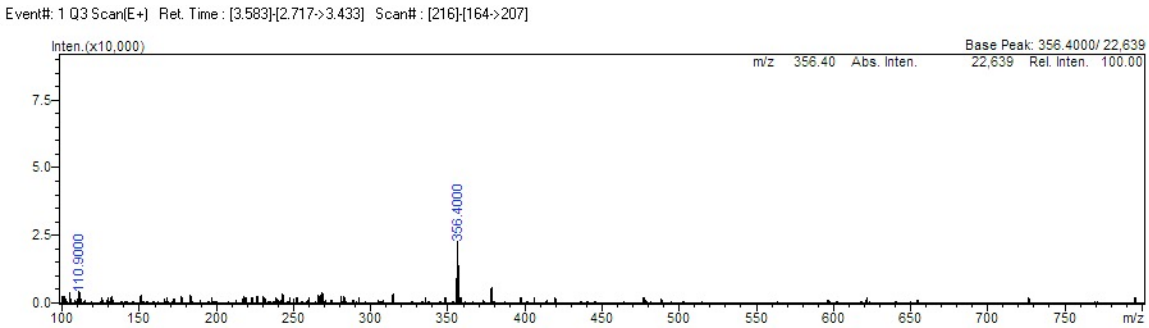

ESI-MS of **SEA-SC1**

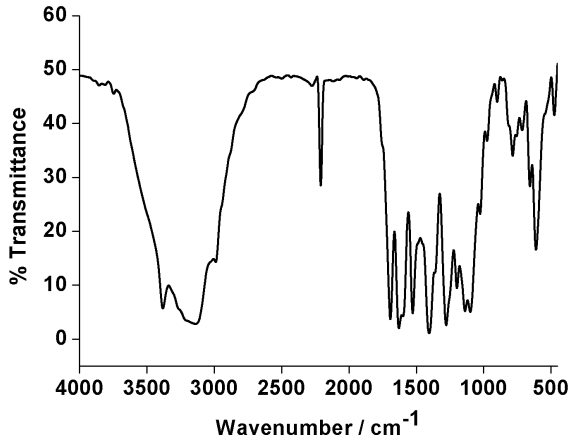

IR spectrum of **SEA-SC1**

Methods and Instruments

NMR spectra: NMR spectra were recorded on a JEOL ECX 400 instrument at 400 MHz for ^{1}H and at 100 MHz for ^{13}C NMR, using tetramethylsilane as an internal standard.

IR Spectra: IR spectra were recorded in the mid IR range of 4000–450 cm^{-1} on a PerkinElmer spectrophotometer by making KBr pellets and expressed as wavenumber (cm^{-1})

LC-MS: LC-MS was recorded by using a Shimadzu HPLC with a Kinetex 1.7 μm XB-C18 (50 x 2.1 mm) column coupled with a UV-Vis detector and mass spectrometer (ESI, Shimadzu). Solvents: 0.1% formic acid in MeCN (sol. A) and 0.1% formic acid in H_2O (sol. B); Method: blinear elution gradient for A/B (5/95): 0 to 1 min, A/B (90/10): 1 to 7 min, A/B (5/95): 7 to11 min; Flow rate: 0.5 mL/min.

All the absorption, emission, DLS and HPLC measurements were carried out three times. The graphs have been prepared with the average value and the error bars have been also incorporated accordingly.

Absorption spectroscopy: Absorbance spectra were measured using UV-Vis spectrometer (UV-2450, Shimadzu) within 400-800 nm wavelength range. The path length was 1 cm for all the measurements.

Calculation of molarity of gold nanoparticle solutions: Concentration of gold nanoparticles calculated according to our recent report (reference 20 in manuscript).

Transmission Electron Microscopy (TEM): The TEM images of gold nanoparticles were performed using FEI, Technai G2 20 S-TWIN. Gold nanoparticles solutions were placed in carbon-coated copper grids with 200 mesh obtained from Icon Analytical.

NIR Luminescence spectroscopy: NIR luminescence spectra were measured using FLS-980 Edinburgh Instrument within 800-1200 nm wavelength range. Excitation and emission bandwidth of equipment was kept at 15 nm.

Relative quantum yield (QY) measurement: FLS-980 Edinburgh Instrument used for QY measurement. Relative QYs of the nanomaterials have been measured in relative scale with respect to Au-4 sample from our recent report (reference 20 in manuscript).

Fluorescence Spectroscopy: Fluorescence spectra of fluorophores were monitored using Synergy Micro plate Reader (BIOTEK USA) within 500-700 nm wavelength range. The bandwidth of equipment was kept at 16.0 nm for both excitation and emission.

DLS measurement: Gold nanoparticle solution and cryptand solution have been filtered through a 0.2 micron filter before the DLS experiment. These filtered solutions have been used in the measurements. Zetasizer Nano ZS90 (Malvern Instruments) used to measure the hydrodynamic diameters of the gold nanoparticles. DTS applications 7.03 software was used to analyze the data. All sizes reported here were based on intensity average. Two DLS measurements were conducted for each sample with a fixed 11 runs and each run lasts 10 s.

Field Emission Scanning Electron Microscope (FE-SEM): The FE-SEM (MIRA3 TESCAN) was employed to analyze the morphological aggregation features where all the samples were prepared by drop casting the solution in silicon wafers.

HPLC Analysis: Recovery of both fluorophores from their complexes with **AuSS** was monitored using an Agilent 1200 Infinity series HPLC equipped with DAD and with a Agilent Eclipse Plus C18 (4.6 × 250 mm, 5µm) column (linear gradient from 65% H_2O 0.1% formic acid to 90% MeCN 0.1% formic acid in 30 minutes with a flow rate of 1 mL/min).

Guest uptake calculation for Table 1: Number of guests per supraparticle and guest occupied void space have been calculated as per literature method (reference 6 in manuscript). The supraparticles have been washed thoroughly with the same solvent to avoid the guests, which were adhered to the surface of the supraparticles. This process has been repeated three times and calculations have been reported on the basis of the average data (± 5%). In this calculation, we have considered that the each gold nanoparticle size does not alter in presence of cryptand. The number of gold nanoparticles in one $\mathbf{AuSS_L}$ particle has been found to be 3.43×10^7. For elongated dodecahedron volume has been calculated from the equation: $V = 6a^3$, where a = edge length. The number of gold nanoparticles in one $\mathbf{AuED_L}$ particle has been found to be 2.59×10^7. The van der Waal's volume of **SEA-SC1** is 0.36 nm^3, which has been calculated as per the same literature method (reference 6 in manuscript). Molar concentration of guest/host has been calculated via dividing the no. of moles of guest molecules per supraparticle by the volume (L) of the suprasparticle host.

Supporting Figures

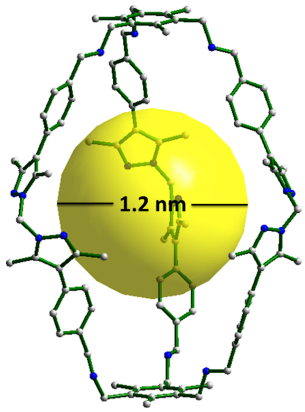

Figure S1. Crystal structure of cryptand**1**

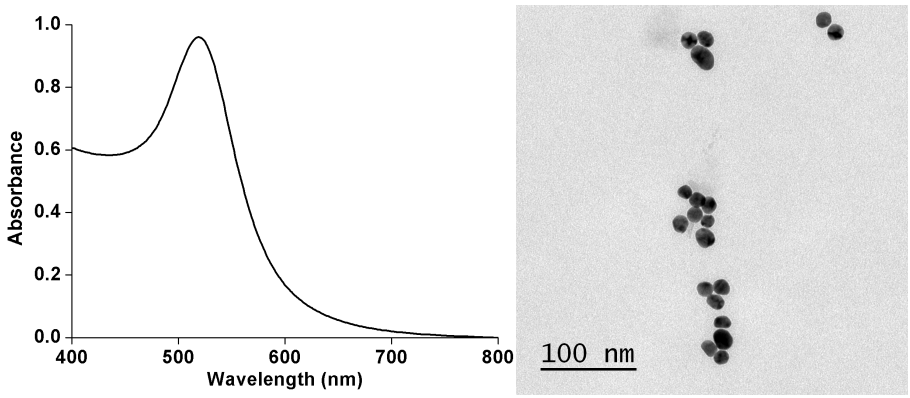

Figure S2. Absorbance spectrum (left) and TEM image (right) of **AuNP.**

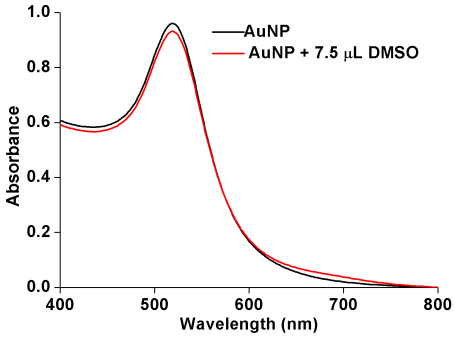

FigureS3. Absorbance spectra of 0.8 nM **AuNP** after addition of DMSO.

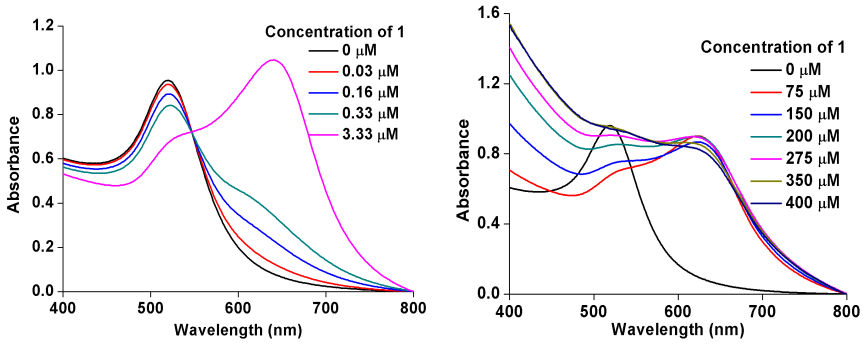

Figure S4. Absorbance spectra of 0.8 nM **AuNP** after addition of **1**

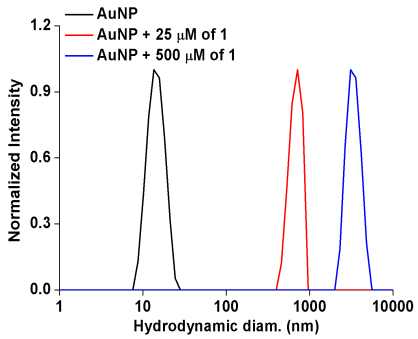

FigureS5. Hydrodynamic diameter of 0.8 nM **AuNP** after addition of **1.**

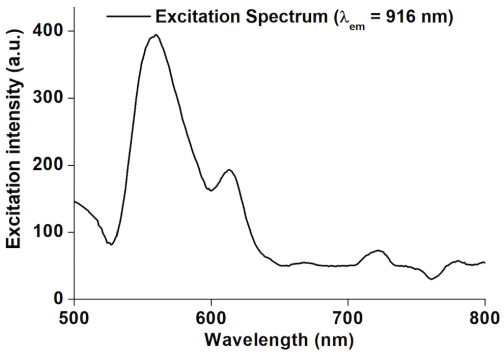

Figure S6. Excitation spectrum after addition of **1** to AuNP.

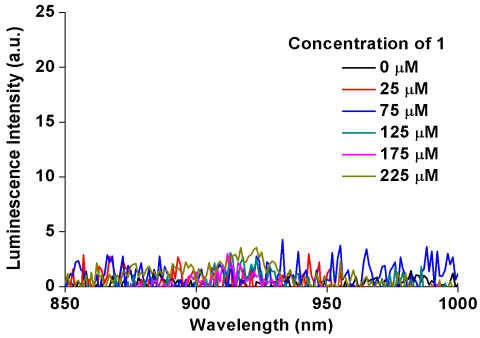

Figure S7. Emission spectra of **1** at different concentration.

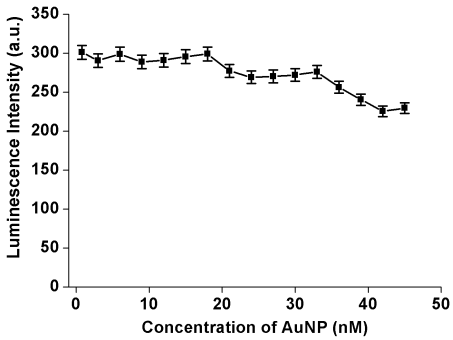

Figure S8. Emission intensity variation with AuNP concentrationin presence of 500 μM cryptand **1.** The lines have been drawn as guide for eyes.

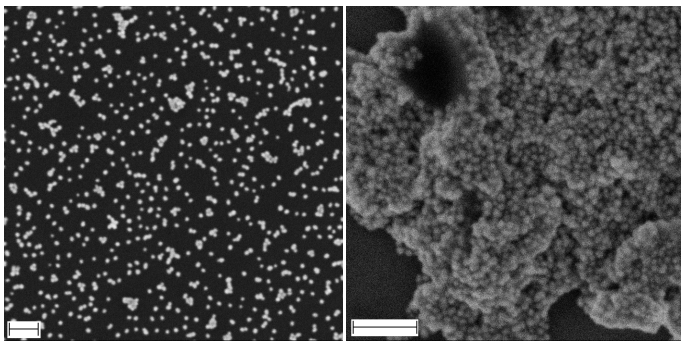

Figure S9. FE-SEM of **AuNP** before (left) and after (right) addition of 25 μM cryptand **1**. Scale bar 100 nm.

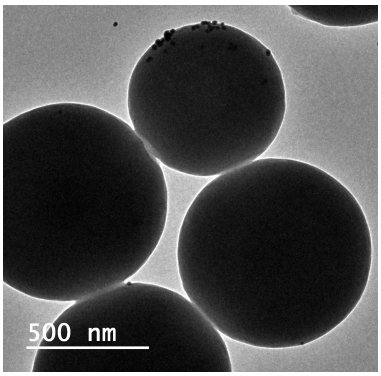

Figure S10. TEM images of **AuNP** after addition of 500 μM cryptand **1**.

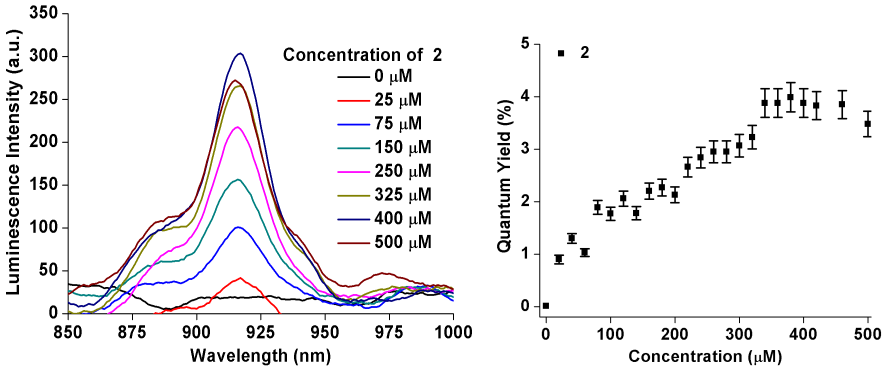

Figure S11. Luminescence spectra (left) and quantum yield (right) of 0.8 nM **AuNP** after addition of **2** at different concentration.

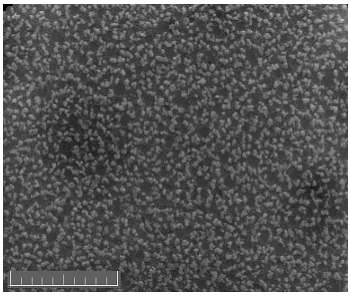

Figure S12. FE-SEM of **AuNP** after addition of 25 μM cryptand **2**. Scale bar 2 μm.

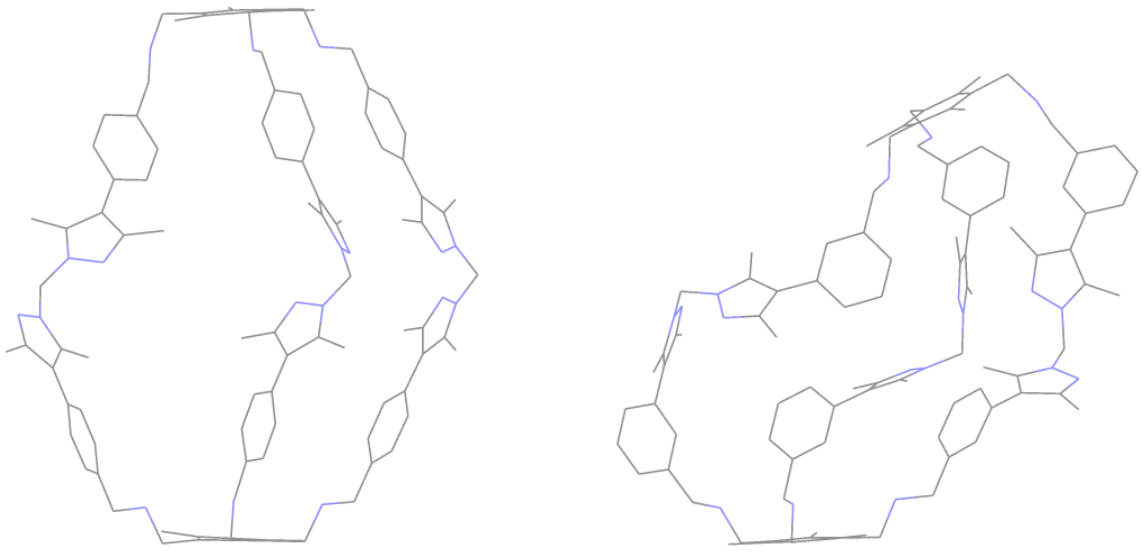

Figure S13. The energy-minimized ground state geometries of cryptand **1** (left) and **2** (right) obtained from B3LYP/6-31G++ level of theory using the Gaussian 09 program package.[S4] The hydrogen atoms have been removed from these diagram for clarity of the cryptand geometries.

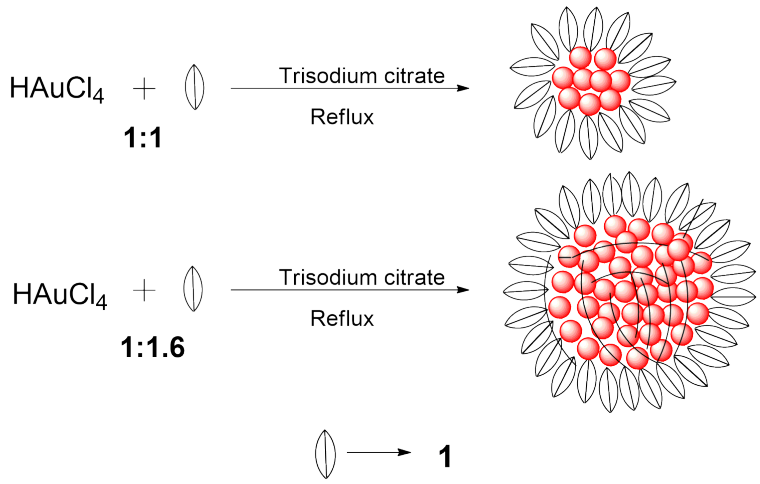

Scheme S1. In situ syntheses of **Au_1** and **$AuSS_{NL}$** with cryptand **1** via citrate based reduction.

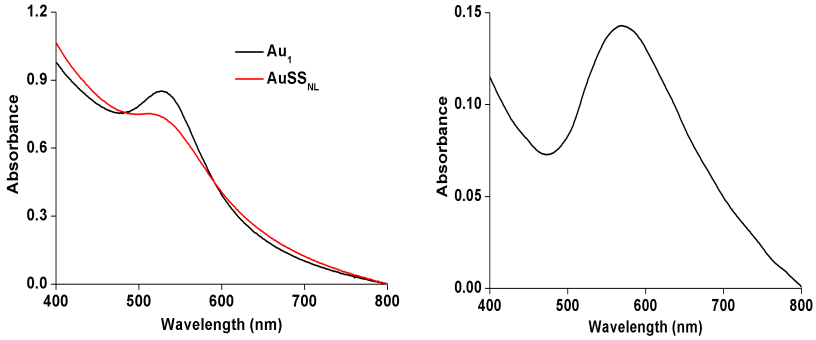

Figure S14. Absorbance spectra of **Au_1**, **$AuSS_{NL}$** (left) and **$AuLS_{NL}$** (right).

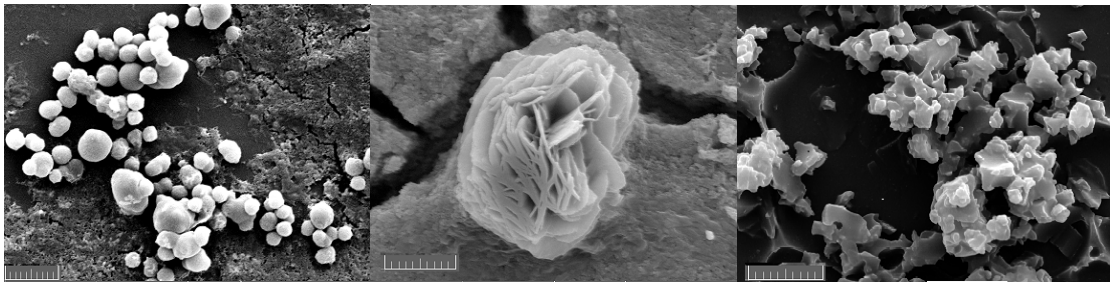

Figure S15. FESEM images of **Au_1**, **$AuSS_{NL}$** and **$AuLS_{NL}$**. Scale bar 2 µm.

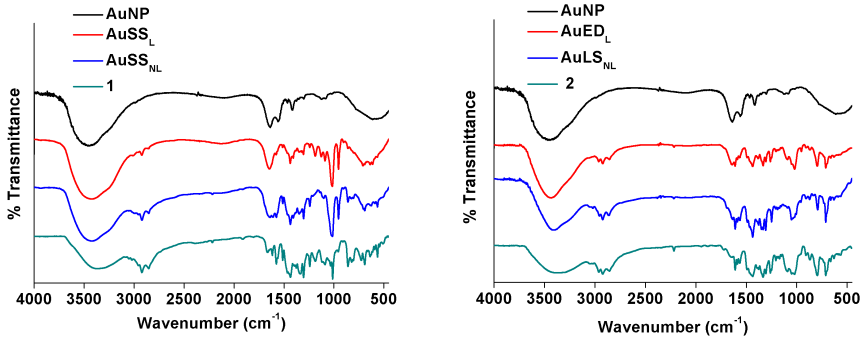

Figure S16. IR spectraof **AuNP, $AuSS_L$, $AuSS_{NL}$** and **1** (left) and **AuNP, $AuED_L$, $AuLS_{NL}$** and **2** (right).

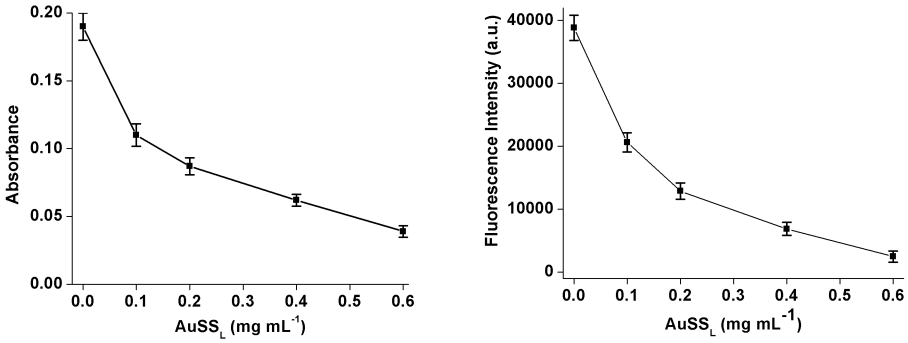

Figure S17. Change in absorbance (left) and fluorescence (right) intensities of 10 μM fluorescein solution with different amount of **AuSS$_L$**. The lines have been drawn as guide for eyes.

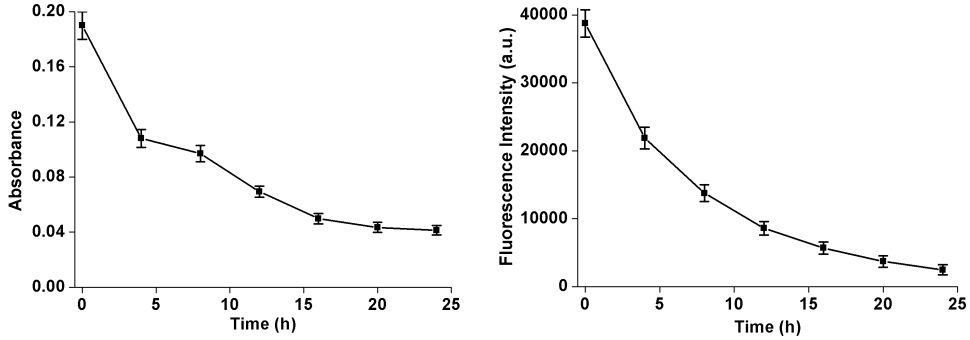

Figure S18. Time dependent absorption (left) and emission (right) intensities of 10 μM fluorescein in presence of **AuSS$_L$** (conc. of **AuSS$_L$** = 0.6 mg/mL). The lines have been drawn as guide for eyes.

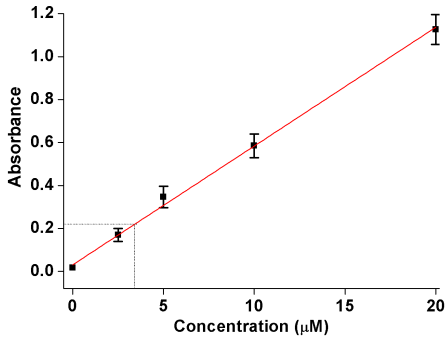

Figure S19. Absorbance based fluorescein recovery by acetic acid treatment to **fluorescein-AuSS$_L$** and compared with calibrated data.

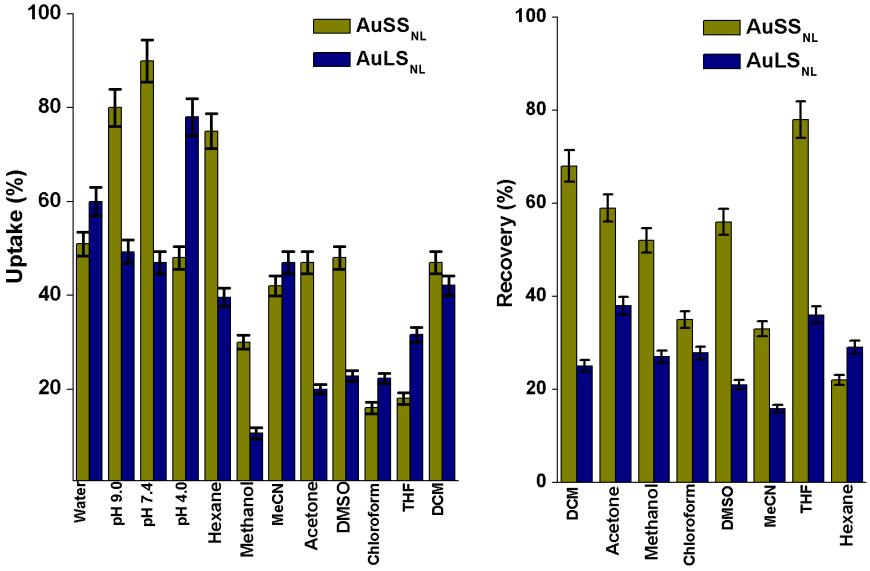

Figure S20. Uptake of **SEA-SC1** in different solvents after 24 h treatment with **AuSS$_{NL}$** and **AuLS$_{NL}$** (left) and recovery of **SEA-SC1** after the addition of organic solvent to the **SEA-SC1-AuSS$_{NL}$** and **AuLS$_{NL}$** prepared in aqueous medium (right).

References:

S1 A. V. Virovets, D. A. Piryazev, E. V. Lider, A. I. Smolentsev, S. F. Vasilevskii, L. G. Lavrenova, *J. Struc. Chem.* 2010, **51**, 92.

S2 A. W. Van der Made, R. H. J. Van der Made, *Org. Chem.*1993, **58**, 1262.

S3 K. J. Wallace, R. Hanes, E. Anslyn, J. Morey, K. V. Kilway, J. Siegel, S*ynthesis* 2005, 12.

S4 Gaussian 09, Revision **E.01**, M. J. Frisch, G. W. Trucks, H. B. Schlegel, G. E. Scuseria, M. A. Robb, J. R. Cheeseman, G. Scalmani, V. Barone, B. Mennucci, G. A. Petersson, H. Nakatsuji, M. Caricato, X. Li, H. P. Hratchian, A. F. Izmaylov, J. Bloino, G. Zheng, J. L. Sonnenberg, M. Hada, M. Ehara, K. Toyota, R. Fukuda, J. Hasegawa, M. Ishida, T. Nakajima, Y. Honda, O. Kitao, H. Nakai, T. Vreven, J. A. Montgomery, Jr., J. E. Peralta, F. Ogliaro, M. Bearpark, J. J. Heyd, E. Brothers, K. N. Kudin, V. N. Staroverov, R. Kobayashi, J. Normand, K. Raghavachari, A. Rendell, J. C. Burant, S. S. Iyengar, J. Tomasi, M. Cossi, N. Rega, J. M. Millam, M. Klene, J. E. Knox, J. B. Cross, V. Bakken, C. Adamo, J. Jaramillo, R. Gomperts, R. E. Stratmann, O. Yazyev, A. J. Austin, R. Cammi, C. Pomelli, J. W. Ochterski, R. L. Martin, K. Morokuma, V. G. Zakrzewski, G. A. Voth, P. Salvador, J. J. Dannenberg, S. Dapprich, A. D. Daniels, Ö. Farkas, J. B. Foresman, J. V. Ortiz, J. Cioslowski, and D. J. Fox, Gaussian, Inc., Wallingford CT, 2009.